The Astrophysical Journal, 708:450–455, 2010 January 1 doi:10.1088/0004-637X/708/1/450

QUASI-PERIODIC OSCILLATIONS IN LASCO CORONAL MASS EJECTION SPEEDS

A. Shanmugaraju[1], Y.-J. Moon[2], K.-S. Cho[3], S. C. Bong[3], N. Gopalswamy[4], S. Akiyama[4], S. Yashiro[4], S. Umapathy[5], and B. Vrsnak[6]

[1] Department of Physics, Arul Anandar College, Karumathur-625 514, India; shanmugaraju_a@yahoo.com
[2] School of Space Research, Kyung Hee University, Yongin 446-701, Republic of Korea; moonyj@khu.ac.kr
[3] Korea Astronomy and Space Science Institute (KASI), Whaamdong, Yuseong-gu, Daejeon, 305-348, Republic of Korea
[4] NASA Goddard Space Flight Center, Greenbelt, MD, USA
[5] School of Physics, Madurai Kamaraj University, Madurai, India
[6] Hvar Observatory, Faculty of Geodesy, Zagreb, Croatia

Received 2009 August 16; accepted 2009 November 10; published 2009 December 11

ABSTRACT

Quasi-periodic oscillations in the speed profile of coronal mass ejections (CMEs) in the radial distance range 2–30 solar radii are studied. We considered the height–time data of the 307 CMEs recorded by the Large Angle and Spectrometric Coronagraph (LASCO) during 2005 January–March. In order to study the speed–distance profile of the CMEs, we have used only 116 events for which there are at least 10 height–time measurements made in the LASCO field of view. The instantaneous CME speed is estimated using a pair of height–time data points, providing the speed–distance profile. We found quasi-periodic patterns in at least 15 speed–distance profiles, where the speed amplitudes are larger than the speed errors. For these events we have determined the speed amplitude and period of oscillations. The periods of quasi-periodic oscillations are found in the range 48–240 minutes, tending to increase with height. The oscillations have similar properties as those reported by Krall et al., who interpreted them in terms of the flux-rope model. The nature of forces responsible for the motion of CMEs and their oscillations are discussed.

Key words: Sun: corona – Sun: coronal mass ejections (CMEs) – solar wind

1. INTRODUCTION

Coronal mass ejections (CMEs) are magnetized plasma clouds ejected from the Sun through the solar corona and the solar wind. It is assumed that the eruption is driven by the Lorentz force. The observed properties of CME dynamics are explained by various magnetohydrodynamical models, including the flux-rope model (Chen et al. 1997, 2000; Wood et al. 1999; Krall et al. 2001; Chen & Krall 2003).

It has been found that the propagation of CMEs is strongly affected by the ambient solar wind plasma (Lindsay et al. 1999; Gopalswamy et al. 2000, 2001). The influence of aerodynamic drag force on CME propagation has been studied by several authors (Vrsnak 2001; Vrsnak & Gopalswamy 2002; Vrsnak et al. 2004; Cargill 2004) and they found that CMEs traveling at velocities lower than the ambient solar wind speed are accelerated, whereas CMEs propagating with higher speeds are decelerated. However, the interplay between the CME speed and the drag due to solar wind is not fully understood. Because the solar wind is accelerated in the range 2–30 $R_{\odot}$, its speed is not uniform (Sheeley et al. 1997). Also, the residual acceleration of CMEs occurs in this range (Zhang & Dere 2006). Hence, the knowledge of the radial evolution of CMEs in the Large Angle and Spectrometric Coronagraph (LASCO; Brueckner et al. 1995) field of view (FOV) is important for the understanding of both the ambient solar wind and the dynamics of CMEs at these heights.

Recently, Krall et al. (2001) used detailed measurements of 11 CMEs having flux-rope-like morphological signatures, and showed that their behavior is in agreement with theoretically modeled erupting flux-rope dynamics. They concluded that flux-rope CMEs constitute a distinct class of CMEs, characterized by specific morphological and dynamical properties. They also reported oscillatory fluctuations of velocity in several CMEs. As far as we know, this is the only report about the CME velocity oscillations, except for a note in Moon et al. (2004), where the oscillating motions of the CME speed are briefly mentioned (see Figure 3 therein). Krall (2007) later hypothesized that all CMEs are flux ropes.

In this paper, we analyze the speed–distance profiles for a set of CMEs. In a number of cases, we have noticed quasi-periodic oscillations in the speed profile. We performed a detailed analysis of physical properties of these oscillations, focusing on some aspects not included in the study by Krall et al. (2001). For example, we noticed that the oscillations are superposed to an exponential growth of the speed. We have also found an increase of the oscillation periods over height and that is interpreted in terms of Alfvén travel time. In addition, the study provides an insight into the Lorentz force/acceleration for the CMEs analyzed in this paper. Finally, the oscillations are interpreted in terms of an unstable/metastable flux rope launched into the solar wind. In the next section, we describe measurements and summarize the characteristics of these velocity oscillations. Results are discussed in Section 3. Finally, conclusions are presented in Section 4.

2. OBSERVATIONS AND RESULTS

We considered a sample of 307 CMEs observed during 2005 January–March and reported in the LASCO CME online catalog (http://cdaw.gsfc.nasa.gov/CME_list; Yashiro et al. 2004; Gopalswamy et al. 2009). We have chosen this period of declining solar activity, so that the chances of the interaction between CMEs are small. We have considered only the CMEs having at least 10 height–time measurements. After applying this criterion, the sample reduced to 116 events, which we used for further analysis. Unlike in Krall et al. (2001), the selection of CMEs in the present work was not limited to those that exhibited flux-rope-like features.

Table 1
List of CMEs for which the Period of the Quasi-periodic Oscillations are Measured[a]

Date	Time	Duration	Distance	Width	Speed	Acceleration	ΔV	V_{mean}	Period (min) at		
(dd/mm)	(UT)	(hr:min)	$R_\odot$	(deg)	(km s^{-1})	(m s^{-2})	(km s^{-1})	(km s^{-1})	5 $R_\odot$	10 $R_\odot$	15 $R_\odot$
08/01	16:30	10:12	2.94–17.31	122	256	11.2	308	376	72	240	...
09/01	02:30	8:14	2.51–27.82	67	603	7.4	197	555	48	168	192
10/01	18:30	19:12	3.33–28.75	96	251	8.3	352	443	164	168	168
11/01	17:30	9:12	3.38–14.74	21	239	2.2	328	340	120	166	...
13/01	08:54	6:48	2.54–12.13	95	267	−0.7	164	300	72	240	...
30/01	15:54	7:48	2.99–21.78	156	454	8.3	245	429	72	240	240
31/01	16:06	12:12	2.7–23.55	26	553	14.1	271	515	...	...	204
08/02	01:31	5:12	2.66–18.57	43	589	−1.5	435	634	72	192	192
12/02	12:54	8:48	4.88–17.52	42	291	4.3	214	304	120	120	120
06/03	20:59	11:42	3.24–19.35	33	263	5.7	295	409	144	212	168
14/03	08:00	5:18	2.63–25.55	105	849	11.6	157	852	48	84	192
16/03	12:48	7:30	4.46–21.87	23	444	7.6	241	513	48	168	192
21/03	14:36	5:06	2.31–25.87	150	920	−28.6	418	967	48	188	120
27/03	07:00	13:18	3.1–23.71	28	292	6.5	298	407	72	120	240
28/03	04:36	13:42	3.13–18.95	30	223	2	320	270	48	240	240

Note. [a] If there is a blank, it means the period cannot be measured.

2.1. Speed–Distance Profile of CMEs

In the analysis, we have utilized the height–time data reported in the LASCO catalog. Instantaneous speeds of CMEs in the LASCO C2–C3 FOV was determined using two successive height–time measurements,

$$v_i = (\Delta h/\Delta t)_i = (h_{i+1} - h_i)/(t_{i+1} - t_i)\,. \quad (1)$$

The height (h_i) corresponding to a given v_i is taken as $h = (h_i + h_{i+1})/2$. Then, the speed–distance profile, $v(h)$, is drawn for each event. t_i is the time corresponding to a particular height.

As an example of the described procedure, the speed–distance profiles for two CMEs (2005 January 8 and 10) are shown in Figures 1(a) and (b). For the 2005 January 8 event (the first appearance in LASCO C2 FOV at 16:30 UT), the CME speed around 3 $R_\odot$ was 140 km s^{-1} and increased to nearly 600 km s^{-1} around 17 $R_\odot$. The mean speed and acceleration reported in the LASCO catalog are 256 km s^{-1} and 11.2 m s^{-2}, respectively. Similarly, for the 2005 January 10 event (18:30 UT), the CME speed was 28 km s^{-1} at 3.5 $R_\odot$ and increased to nearly 470 km s^{-1} at 27.5 $R_\odot$. The reported mean speed and acceleration are 251 km s^{-1} and 8.3 m s^{-2}, respectively.

Figures 1(a) and (b) reveal quasi-periodic pattern in the $v(h)$ profile superposed onto an approximately linear increase of the CME speed (h represents the radial distance expressed in units of $R_\odot$). CME speed can be separated into two components,

$$v_{cme} = v_{lin} + v_{osc}, \quad (2)$$

where v_{lin} means that the velocity is a linear function of the distance (non-oscillatory component) and v_{osc} is the oscillatory component. In the velocity–time space, this corresponds to an exponential growth, since $R \propto e^{\omega t}$ implies $v = \dot{h} \propto \omega e^{\omega t}$, i.e., $v = \omega h$ (Vrsnak 2001).

Among the speed–distance profiles of 116 events, we identified two classes of CMEs, either accelerating or decelerating. That is, CMEs followed either $v(h) = v_0 + \omega h$ or $v(h) = v_0 - \omega h$, where v_0 is the initial speed and ω is the growth rate. There are a few cases for which the growth rate was nearly zero. The superimposed oscillating pattern is found in the speed–distance profiles of most of the CMEs. However, it is seen clearly only in 15 events, all being traced over a long distance range. The events are listed in Table 1. The data for these 15 events were smoothed by the spline interpolation, making the oscillating pattern clearer, as illustrated in Figures 2(a) and (b).

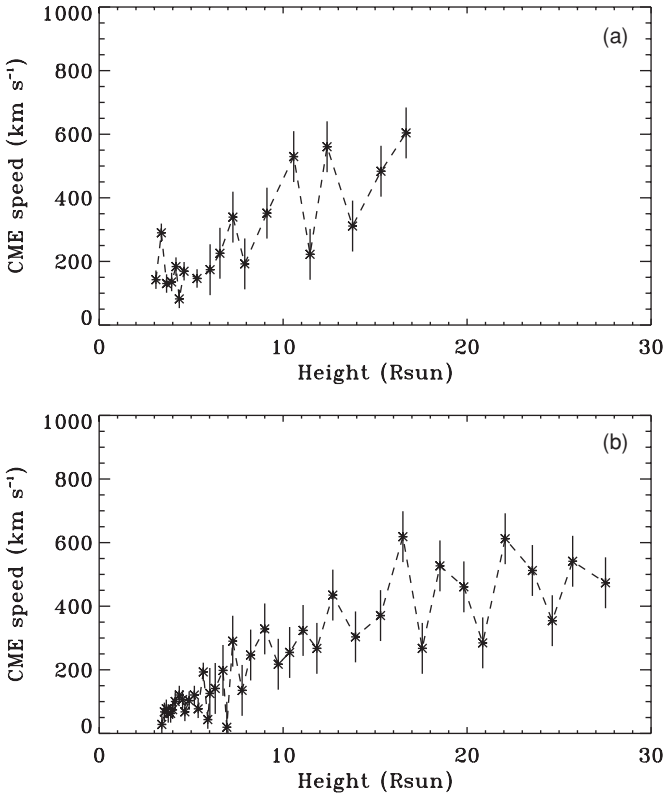

Figure 1. (a) Speed–distance profile of a CME observed on 2005 January 8. (b) Same as above for the CME on 2005 January 10. The error bar shows the speed error obtained for LASCO C2 and C3 coronagraphs.

2.2. Period of Oscillations

Besides the $v(h)$ profiles, we have also analyzed the speed–time profiles, $v(t)$, for all the 15 CMEs, in order to measure the period of oscillations. In Figure 3, we show two examples of smoothed $v(t)$ profiles. The oscillation periods were determined

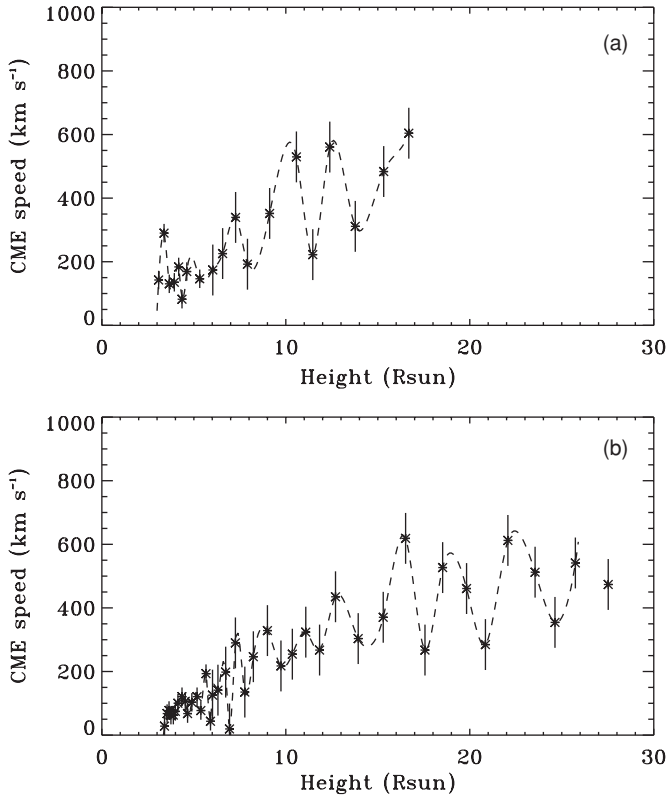

Figure 2. (a) Speed–distance profile of a CME observed on 2005 January 8. Dashed line is the spline interpolation fit to show the oscillation pattern. (b) Same as above for the CME on 2005 January 10.

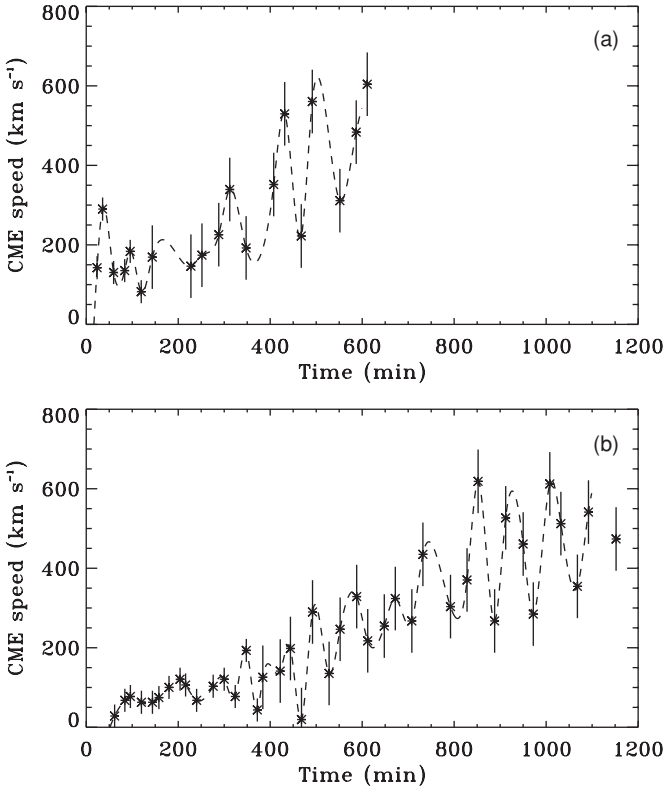

Figure 3. (a) Speed–time profile of a CME observed on 2005 January 8. Dashed line is the spline interpolation fit to show the oscillation pattern. (b) Same as above for the CME on 2005 January 10.

at three different radial distances (5, 10, and 15 $R_\odot$) and are displayed in Table 1. The first three columns of Table 1 show the date, the first appearance time of CMEs in the LASCO C2 FOV, and the duration of the observational interval, respectively. The CME distance range is shown in Column 4. Columns 5–7 show the width, speed, and acceleration of the CMEs. The velocity amplitude (ΔV) and mean speeds ($V_{\rm mean} = (V_{\rm max} + V_{\rm min})/2$) of the CMEs, estimated from the oscillation profile, are given in Columns 8–9. The period (T) of the quasi-periodic oscillations at three different heights is given in the last column.

It can be observed from Table 1 that the oscillation period varies between 48 and 240 minutes. In 10 cases, the oscillation period increases as the CME height increases from 5 $R_\odot$ to 15 $R_\odot$.

Finally, we have obtained the speed–distance profiles for each of the 15 events using three point differences of the height–time data and the quasi-periodic oscillations are still seen. Two examples are shown in Figure 4.

2.3. Speed Error

In order to check whether these oscillations are true, we check whether the oscillation amplitudes are higher than the error in CME speed measurements. The LASCO C2 FOV covers the range 2–6 $R_\odot$. Since the MVI files were used for the CME measurements in the online catalog, the pixel size is 23.″79 for C2 and 112″ for C3. If we adopt that the height error is 23.″79, then the speed error expressed in km s^{-1} would be $\Delta V_{\rm CME} = 2 \times 23.79 \times 725/t_c$, where t_c is the time cadence expressed in seconds. During 2005 January–March, the average time cadence of LASCO C2 images was around 19.7 minutes, thus the speed error can be estimated as 29 km s^{-1}. Similarly, we

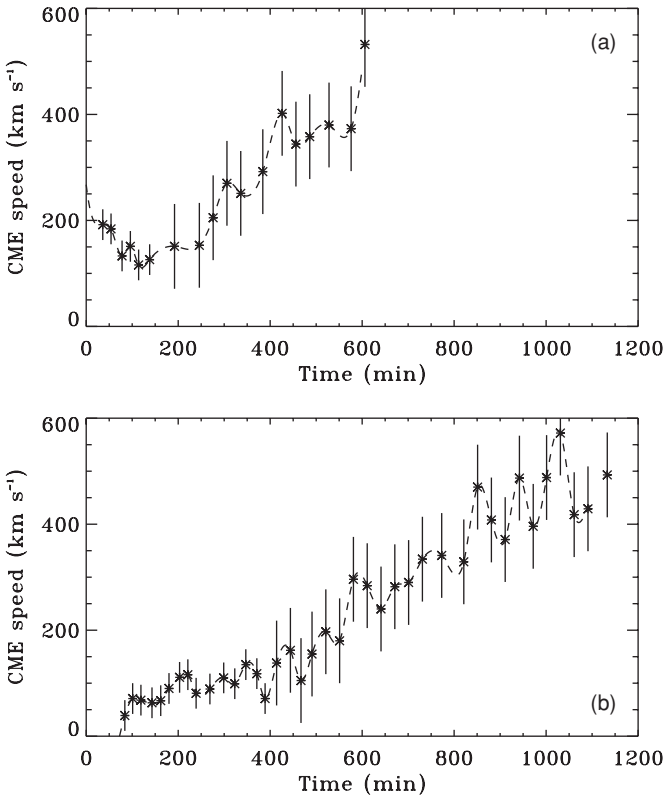

Figure 4. (a) Speed–time profile of a CME observed on 2005 January 8 obtained using three point differences of height–time data. Dashed line is the spline interpolation fit to show the oscillation pattern. (b) Same as above for the CME on 2005 January 10.

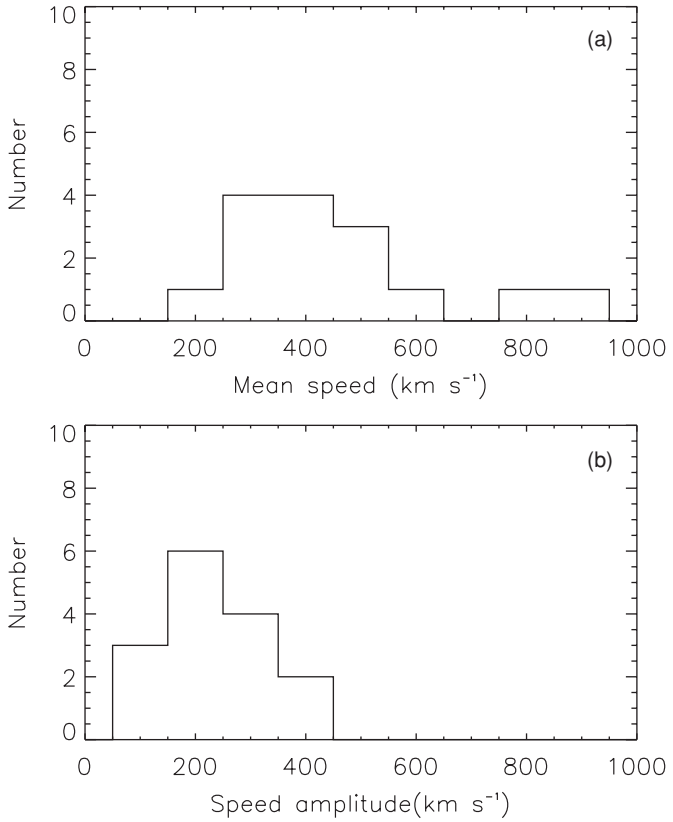

Figure 5. Distribution of the (a) mean speeds and (b) speed amplitudes of the oscillations.

find a speed error of 80 km s^{-1} for the LASCO C3 measurements if we use a resolution of 112″ and 34 minutes time cadence. We also note that according to a recent analysis of errors in LASCO height measurements reported by Wen et al. (2007), a constant error of about 0.25 $R_\odot$ at all heights above 5 $R_\odot$ is probably a good approximation. For a time cadence of 20 minutes, one would get a speed error around 145 km s^{-1}.

The distribution of mean speeds in the oscillation period ($V_{\rm mean} = (V_{\rm max} + V_{\rm min})/2$) of all the 15 events is shown in Figure 5(a). Note that most of the mean values are around 400 km s^{-1}, which is about the solar wind speed. This may be related to the drag effect that is discussed in Section 3.

In our data, we found that the amplitude of the velocity oscillation is larger than the estimated error for all of the 15 events listed in Table 1. The amplitude is larger than 200 km s^{-1} in 11 events (73%), in six events (40%) it is larger than 300 km s^{-1}, and in two CMEs (13%) it is even larger than 400 km s^{-1}. The distribution of velocity amplitudes is presented in Figure 5(b).

3. DISCUSSION

The oscillations analyzed in the present study are similar to those of Krall et al. (2001). Similar to their observation, the pattern might be best observed in slowly evolving flux ropes. For example, the morphology of the slowly erupting CME observed on 2005 January 10 (Figure 6) can be related to flux-rope configuration. The two ends of the circular magnetic loop stay anchored to the Sun even up to a distance of 25 $R_\odot$. This CME is a slow event with a mean speed of 250 km s^{-1}. As Krall et al. (2001) suggested, when the geometry of the flux rope changes continuously, the oscillations are likely to change

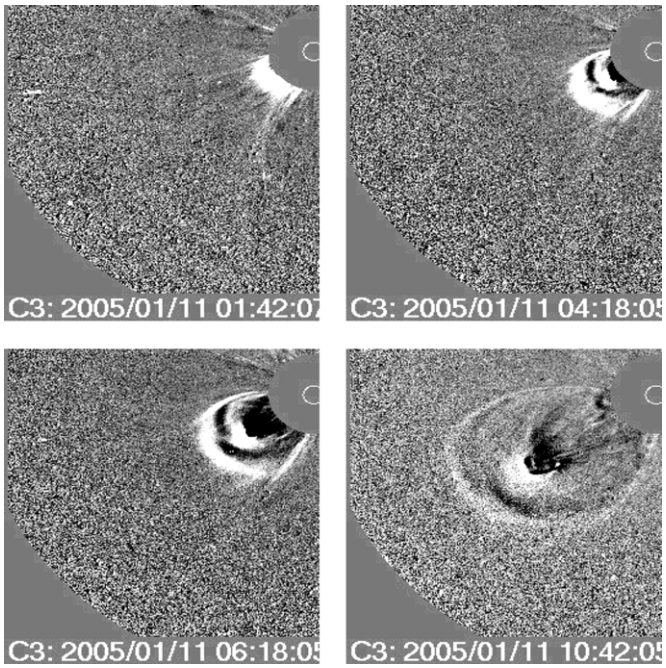

Figure 6. *SOHO*/LASCO C3 images of the CME of 2005 January 10.

in character as the flux rope expands. In agreement to this, the periods of the oscillations of our CMEs tend to increase as the distance increases. It should be noted that from the point of view of the flux-rope model, the eigenmode oscillations are expected when the drive mechanism is too weak to cause an eruption, or if the stable flux-rope configuration is weakly perturbed from equilibrium (Vrsnak 1984; Chen 1989; Vrsnak 1990; Cargill et al. 1994).

The oscillation period with respect to the distance, $T(R)$, is plotted in Figure 7. In the graph, we have compared the measured oscillation period with the period of the loop oscillations due to a standing Alfvén wave,

$$T \approx L/V_A, \tag{3}$$

where V_A is the Alfvén speed and L is the length of the coronal loop $L \approx 2\pi h = 2\pi(R-1)$, i.e., the oscillation period is of the order of the Alfvén travel time. Here, the dominant factor is L, since the value of V_A should not change too much because in the CME expansion both the CME density and CME magnetic field decrease with height. For two different Alfvén speeds (3000 and 500 km s^{-1}), the period is calculated using the above formula and shown in Figure 7. For $V_A = 1000$ km s^{-1}, at $R = 5$ $R_\odot$ we get $T \approx 50$ minutes, and $T \approx 160$ minutes at $R = 15$ $R_\odot$. For lower V_A, periods become too large.

In order to study the nature of forces causing the described oscillations, we have examined acceleration time profiles of our CMEs, applying the two-point difference method. Using the speed–time data, we obtained the acceleration–time profile $a(t)$, as shown in Figure 8. As seen in these graphs, the overall acceleration has oscillating pattern. Actually, in the LASCO FOV (2–30 $R_\odot$), the main acceleration phase might be over for most of CMEs (Zhang & Dere 2006). Generally, only the residual acceleration remains in this range. Hence, the motion of CMEs is governed mainly by the solar wind drag (a_d), gravitational force ($g = 274/R^2$), and any residual acceleration due to the Lorentz force (a_L):

$$a_n = a_L - g - a_d = a_L - g - \gamma(v - w)\,, \tag{4}$$

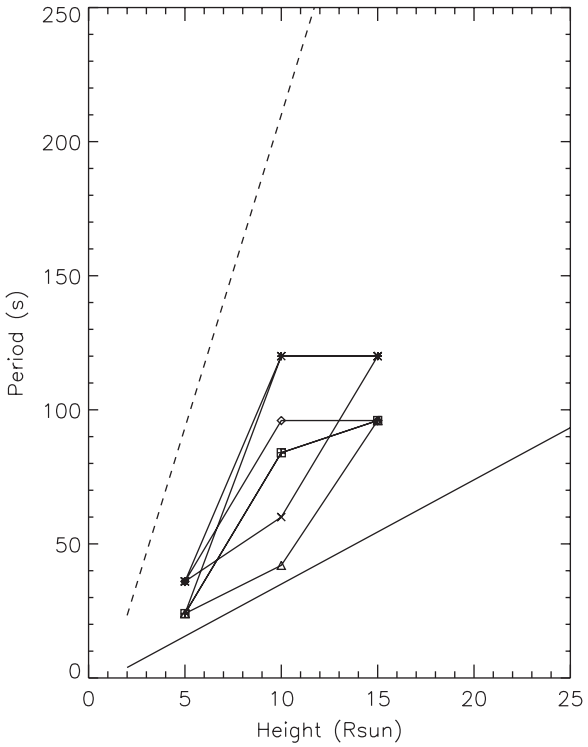

Figure 7. Period of the quasi-periodic oscillations for several events are shown (lines with symbols). Superimposed is the period of the loop oscillation due to Alfvén standing wave: dashed line, $V_A = 500$ km s^{-1}; solid line, $V_A = 3000$ km s^{-1} (see the text for more details).

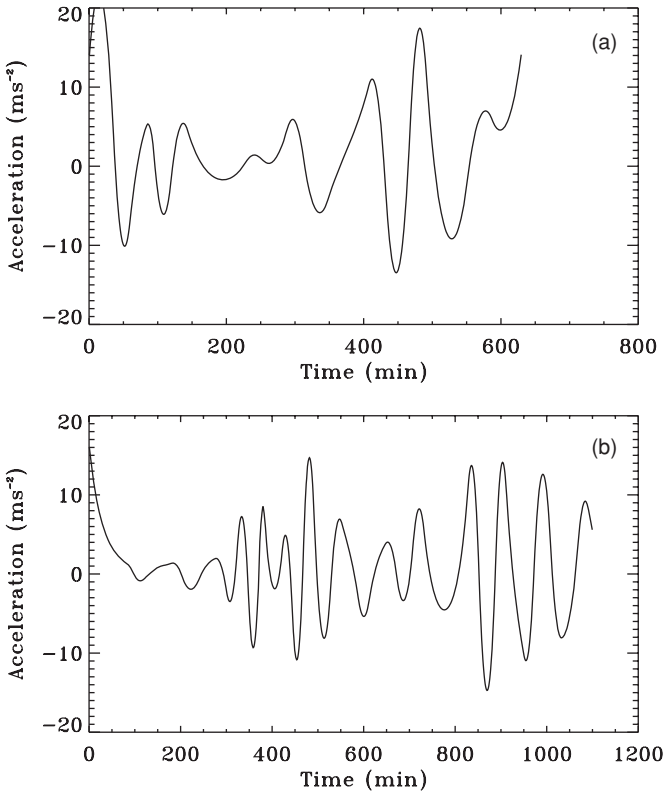

Figure 8. Acceleration–time profile of the two CMEs presented in Figure 1.

where we have used a linear approximation for the drag, $\gamma(v - w)$. Since the CME velocity and the net acceleration at various distances are known for our data, one can obtain the Lorentz force. In order to calculate the Lorentz force for our CMEs, we use the solar wind empirical model proposed by Sheeley et al. (1997):

$$w(R) = w_0\sqrt{1 - e^{-(R-R_1)/R_2}}, \quad (5)$$

where $R_1 = 2.8$ and $R_2 = 8.1$, and we adopted the asymptotic wind speed $w_0 = 400$ km s^{-1}.

Utilizing the empirical scaling for the drag parameter γ as given by Vrsnak (2001), $\gamma = 1.16\ R^{-1.35} \times 10^{-3}$ s^{-1}, we have estimated the variation of the Lorentz force in the LASCO FOV using Equation (4). The results are shown in Figure 9 for CMEs of 2005 January 8 and 10. In this figure, the accelerations due to gravitation (g), drag (a_d), and net acceleration from Figure 8 (a_n) are also shown for comparison. Since the oscillation is present in the velocity profile of the CME, the drag also shows oscillating pattern. Due to the oscillating pattern in the net acceleration, it is also present in the Lorentz acceleration. As seen in this figure, the acceleration due to Lorentz force seems to be of same magnitude as other forces.

Furthermore, we examined a list of 30 events (reported during the period 1999–2006) whose heights were measured in at least 30 coronagraphic images and were characterized by a high-quality index ($\geqslant$4). Almost all of them display the same kind of quasi-periodic oscillations in their speed–distance profile.

The quasi-periodic oscillations in the velocity profile of CMEs can be explained by the flux-rope model when the driving Lorentz force is weak. Depending on the interplay of the Lorentz force and the gravity, an unstable (or metastable) flux rope in the solar atmosphere can jump to an upper equilibrium position

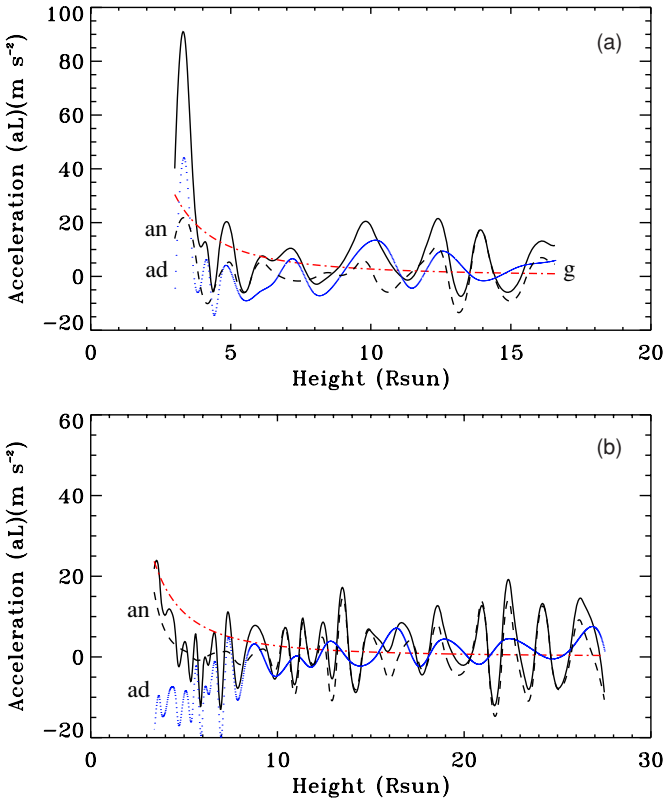

Figure 9. Lorentz acceleration (wavy solid gray line) estimated by assuming the solar wind model with an asymptotic speed of 400 km s^{-1} and using an empirical relation for drag coefficient. The accelerations due to gravitation (g: monotonously decreasing dash-dotted red line), drag (a_d: wavy dotted blue line), and net acceleration from Figure 8 (a_n: wavy dashed line) are also shown.

(e.g., Vrsnak 1990, 2008; Torok & Kliem 2005; for observations, see Vrsnak et al. 1990; Vrsnak 2001). In the absence of the solar wind the flux rope is expected to show a damped oscillation at this upper equilibrium (Vrsnak 2001). However, if the upper equilibrium position is at heights where the solar wind becomes effective, i.e., if the Lorentz force drives the rope into the solar wind, the rope starts to feel the solar wind drag, which continues to drive it into interplanetary space. Thus, instead of oscillating around a fixed height, the rope oscillates while propagating outward. Furthermore, it is expected that the period of eigenmode oscillations increases since the size of the structure increases.

Note that the interpretation according to which some slow CMEs are driven by the solar wind, i.e., that they passively trace the solar wind outflow, was put forward by Sheeley et al. (1997). The idea was founded on the fact that the kinematics of some CMEs is similar to the kinematics of small-scale transient features observed in the LASCO FOV, for which it was demonstrated to be consistent with an isothermal solar wind expansion at a temperature of 1.1 MK and a sonic point near 5 $R_{\odot}$. On the other hand, the idea about existence of an upper equilibrium position, failed eruptions, and oscillations at the upper equilibrium was put forward by Vrsnak (1990) and observationally demonstrated by Vrsnak et al. (1990). In this paper for the first time these two aspects are combined, to explain the oscillatory expansion of slow CMEs.

4. CONCLUSION

We have analyzed the speed–distance profile of a sample of 116 CMEs which have at least 10 height measurements in the *Solar and Heliospheric Observatory* (*SOHO*)/LASCO range of 2–30 $R_{\odot}$. Using these data, we have obtained the speed–distance profile for all the CMEs. We found quasi-periodic oscillations in 15 cases and we have determined their periods and amplitudes. The periods of these quasi-periodic oscillations range between 48 and 240 minutes. The amplitudes of oscillations are higher than the typical error in the CME speed measurements, suggesting that the oscillations are real. The properties of oscillations are similar to that reported by Krall et al. (2001). The oscillations are seen mainly when the CMEs are observed over long distances. The origin of such oscillations can be explained in the scope of the flux-rope model.

We thank the referee for his/her comments on this paper. This work has been supported by the "Development of Korean Space Weather Center" of KASI and KASI basic research funds. Y.J.M. has been supported by the WCU grant (No. R31-10016) funded by the Korean Ministry of Education, Science and Technology, and by the Korea Research Foundation Grant funded by the Korean Government (MOEHRD, Basic Research Promotion Fund; KRF-2008-314-C00158, 20090071744). This CME catalog is generated and maintained at the CDAW Data Center by NASA and The Catholic University of America in cooperation with the Naval Research Laboratory. *SOHO* is a project of international cooperation between ESA and NASA.

REFERENCES

Brueckner, G. E., et al. 1995, Sol. Phys., 162, 357
Cargill, P. J. 2004, Sol. Phys., 221, 135
Cargill, P. J., Chen, J., & Garren, D. A. 1994, ApJ, 423, 854
Chen, J. 1989, ApJ, 338, 453
Chen, J., & Krall, J. 2003, J. Geophys. Res., 108, 1410
Chen, J., et al. 1997, ApJ, 490, L191
Chen, J., et al. 2000, ApJ, 533, 481
Gopalswamy, N., Lara, A., Yashiro, S., Kaiser, M. L., & Howard, R. A. 2001, J. Geophys. Res., 106, 29207
Gopalswamy, N., Yashiro, S., Michalek, G., Stenborg, G., Vourlidas, A., Freeland, S., & Howard, R. 2009, Earth Moon Planets, 104, 295
Gopalswamy, N., et al. 2000, Geophys. Res. Lett., 27, 145
Krall, J. 2007, ApJ, 657, 559
Krall, J., et al. 2001, ApJ, 562, 1045
Lindsay, G. M., Luhmann, J. G., Russell, C. T., & Gosling, J. T. 1999, J. Geophys. Res., 104, 12515
Moon, Y.-J., et al. 2004, ApJ, 615, 1011
Sheeley, N. R., et al. 1997, ApJ, 484, 472
Torok, T., & Kliem, B. 2005, ApJ, 630, L97
Vrsnak, B. 1984, Sol. Phys., 84, 289
Vrsnak, B. 1990, Sol. Phys., 129, 295
Vrsnak, B. 2001, J. Geophys. Res., 106, 25249
Vrsnak, B. 2008, Ann. Geophys., 26, 3089
Vrsnak, B., & Gopalswamy, N. 2002, J. Geophys. Res. 107, 1019
Vrsnak, B., Ruzdjak, V., Brajsa, R., & Zloch, F. 1990, Sol. Phys., 127, 119
Vrsnak, B., Ruzdjak, D., Sudar, D., & Gopalswamy, N. 2004, A&A, 423, 717
Wen, Y., Filipe Maia, D. J., & Wang, J. 2007, ApJ, 657, 1117
Wood, B. E., et al. 1999, ApJ, 512, 484
Yashiro, S., Gopalswamy, N., Michalek, G., St. Cyr, O. C., Plunkett, S. P., Rich, N. B., & Howard, R. A. 2004, J. Geophys. Res. 109, A07105
Zhang, J., & Dere, K. P. 2006, ApJ, 649, 1100